ISSN 0020-4412, Instruments and Experimental Techniques, 2016, Vol. 59, No. 2, pp. 231–238. © Pleiades Publishing, Ltd., 2016.
Original Russian Text © E.G. Krastelev, Yu.D. Kalashnikov, 2016, published in Pribory i Tekhnika Eksperimenta, 2016, No. 2, pp. 76–83.

ELECTRONICS AND RADIO ENGINEERING

A High-Power Generator of Nanosecond Pulses with an Amplitude of up to 500 kV and a Repetition Rate of up to 50 Hz

E. G. Krastelev[a]* and Yu. D. Kalashnikov[b]

[a] *Joint Institute for High Temperatures, Russian Academy of Sciences, Izhorskaya ul. 13/2, Moscow, 125412 Russia*

[b] *RZK Engineering Ltd., Panfilovskii pr. 4/1, Zelenograd, Moscow, 124460 Russia*

* *e-mail: ekrastelev@yandex.ru*

Received February 12, 2015

Abstract—A pulsed-power high-voltage generator, which is combined with an electric-discharge chamber, is designed for selective disintegration of quartz raw minerals and other nonconductive natural and artificial materials. The main parameters of the generator are as follows: the voltage-pulse amplitude, up to 500 kV; the discharge-current amplitude, up to 30 kA; the duration of current pulses (the half-period an oscillatory discharge), 70–90 ns; and the pulse repetition rate, up to 50 Hz. The generator is characterized by a high efficiency, a long service life, the possibility of long continuous operation, and the fulfillment of the electromagnetic compatibility requirements. The experience of the operation of three constructed installations testifies to their high reliability: the number of accumulated pulses in a typical mode (450 kV, 20 Hz) exceeded 10^8 pulses without a repair or replacement of units.

DOI: 10.1134/S0020441216010243

INTRODUCTION

Electric-discharge methods for disintegrating quartz raw materials attract ever increasing attention in connection with a high selectivity of opening minerals along the crystal-cohesion boundaries, liquid–gaseous inclusions, and other inhomogeneities and with the possibility of obtaining high-quality concentrates using ecologically pure methods [1]. One of the key aspects in the solution of this problem is the development of high-power high-voltage (HV) pulse generators with parameters that correspond to the requirements of electric-discharge technologies; such generators must have a long service life to provide long-term continuous operation.

The specific requirements imposed on the generator parameters are determined by the character of its load, for which a discharge channel in a liquid (water) or solid is used.

At the initial fragmentation stages of a lump material that disintegrates to characteristic sizes of several millimeters, the electric-pulse mode with a breakdown through a solid is most efficient [2]. The voltage amplitude that is required for breaking down a lump material is at least 250–300 kV. In this case, one of the determining conditions for embedding the discharge channel into a solid, which is placed in a liquid, is a high voltage-rise rate of at least 10^{12} V/s [3].

The further comminution occurs in a shock-wave mode with the discharge passage in water with the processed material; within the delay time, the high voltage must be maintained across the interelectrode gap of the crushing chamber. The delay of a breakdown of the gap with a length of several centimeters depending on the electrode geometry may reach a few microseconds at voltages of 300–400 kV [4].

After a breakdown in a solid or liquid, the plasma-channel resistance rapidly decreases to several ohms or less within a short time (100–200 ns), within which the main portion of energy is deposited into the discharge channel [5]. A necessary condition for the efficient energy deposition is a low internal impedance of the generator.

The enumerated requirements are provided to the highest degree by pulse generators with an output stage in the form of a capacitive storage, which is charged to the full operating voltage and then is discharged through a switch and a low-inductance transmission line through the working gap of the crushing chamber. This solution provides a high rise rate of the voltage across the gap, maintenance of this voltage for the

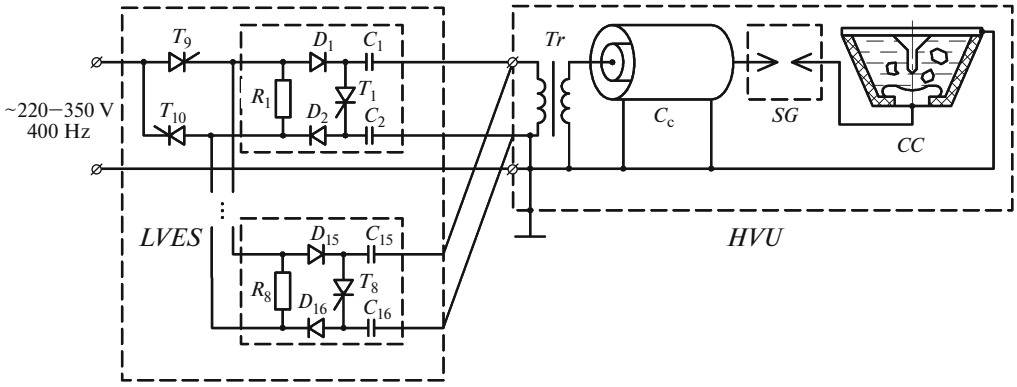

Fig. 1. The circuit diagram of the generator: (*LVES*) low-voltage energy storage; (*HVU*) high-voltage unit; (*Tr*) pulse step-up transformer; (*SG*) gas-filled SG; (*CC*) crushing chamber; and (C_c) high-voltage coaxial capacitor.

breakdown-delay time, and obtaining of current pulses of nanosecond duration after the breakdown [6].

Below, we describe the design of the generator with an HV energy storage, a pulse step-up transformer, and an HV capacitor in the form of a section of a coaxial line, which is discharged through the gap of the crushing chamber. The generator is characterized by a high efficiency, the possibility of long-term continuous operation, a long service life, and high reliability.

THE GENERATOR SCHEME AND DESIGN

Generator Circuit Diagram

The simplified electric circuit of the generator is shown in Fig. 1.

The generator includes a low-voltage primary capacitive energy storage on capacitors C_1–C_{16}, a switch on thyristors T_1–T_8, a step-up pulse transformer *Tr*, a HV capacitor C_c in the form of a coaxial-line section, an output spark-gap switch *SG*, and an electric-discharge crushing chamber *CC*.

The capacitors of the primary storage are charged from the primary-voltage source through the charging switch based on thyristors T_9, T_{10} and rectifying diodes D_1–D_{16}. After the charging terminates, the thyristors T_1–T_8 are enabled and the voltage of the capacitor pairs is applied to the primary winding of the pulse transformer, which transfers the stored energy to the HV capacitive storage—the coaxial capacitor C_c. The formation of a HV pulse with a subsequent breakdown and a current flow in the electric-discharge crushing chamber occurs in response to the operation of one gas-filled spark-gap (SG) switch, which is installed in the circuit between the HV capacitor and the chamber.

The primary capacitive storage and its charging and switching circuits constitute the low-voltage part of the generator. The pulse transformer, the coaxial capacitor, and the output SG with the working chamber constitute the HV section. The elements of the low-voltage generator section are mounted in standard electrotechnical cabinets, and the elements of the HV section are placed in a separate unit and insulated with transformer oil. They are interrelated via cable lines through which pulses from the low-voltage storage arrive at the primary winding of the step-up pulse transformer in the HV generator section. The presence of flexible transmission lines allows one to change the relative arrangement of the units with consideration for the available room and operating conditions.

Low-Voltage Generator Section

The primary capacitive storage consists of eight identical modules (Fig. 1). Each module includes two oppositely charged capacitors, two rectifying diodes, one damping resistor, and a switching thyristor.

The storage is based on KPI-1-75 pulsed capacitors (75 μF, 1 kV). The certified service life of the capacitors is $\geqslant 5 \times 10^8$ pulses at a reverse voltage of $\leqslant 10\%$. To increase the service life of the capacitors and reliability of the facility operation in the pulse–periodic mode, the charging voltage of the capacitors is limited to 500 V. In this case, the total stored energy in 16 capacitors is 150 J, and the expected lifetime for the actual operational conditions exceeds 5×10^9 charge/discharge cycles. To reduce the time for which voltages are applied to the capacitors and switching thyristors, the generator circuit is characterized by fast pulsed charging.

The capacitive storage is charged for 2.5 ms, which is the duration of one period of a supply-voltage frequency of 400 Hz, via unblocking of the charging switch (T_9 and T_{10}, Fig. 1), which consists of two TChI 100-10 thyristors that are connected in opposite polarities, for this time. In this case, one of the thyristors is enabled during one half-wave and the capacitors of one arm of the modules are charged through the

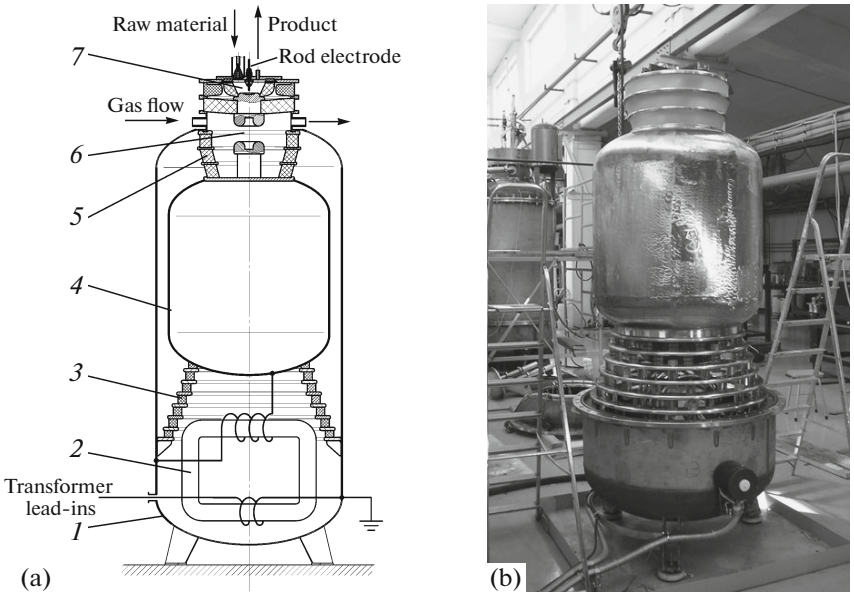

Fig. 2. A schematic image of the HV unit and a photograph of the unit with the removed outer housing: (*1*) case, (*2*) pulse transformer, (*3*) base insulator, (*4*) high-voltage electrode of the coaxial capacitor, (*5*) output insulator, (*6*) gas-filled SG, and (*7*) crushing chamber.

corresponding rectifying diodes; the other thyristor is enabled during the second half-wave, and the capacitors of the second arm are charged through the other group of diodes. Control pulses of the thyristors are generated by the master-generator circuit and are synchronized with the moments when the charging voltage with a frequency of 400 Hz passes through zero.

A PSCh-30 commercial synchronous frequency converter (motor–generator) (400 Hz, 3 × 220 V) is used as the charging-voltage source, thus fully excluding an impulsive load of the supply mains and the penetration of pulse interference into it. To implement the impact operating mode with an impulsive load, the voltage-stabilization circuit of the PSCh-30 generator is replaced by a controlled rectifier of the choke-biasing current in the exciting-winding circuit. Varying the rectifier voltage makes it possible to control the excitation current and, correspondingly, the generator output voltage. This solution allows the implementation of a pulse charging mode of the storage capacitors up the maximum voltage, whose amplitude at the linear generator outputs reaches 500 V.

The charging current of the capacitors is limited by the inductance of the charging circuit. The main contribution to it is made by the self-inductance of the PSCh-30 generator amounting to ~500 μH. At a maximum output voltage with an amplitude of 500 V, the peak value of the charging current is ≈400 A.

The capacitors are discharged some time later (in ~2.5 ms) after the termination of the charging cycle, which is necessary for reliable disabling of the thyristors of the charging switch and termination of all transient processes. Enabling pulses are fed to the switching thyristors T_1–T_8 (TChI100-12) from the common generator through isolating transformers with resistors that are connected in series and restrict the control-current amplitude at a level of 4 A at a pulse duration of ≈10 μs. To protect thyristors against overvoltages, varistors and standard *RC*-chains, which suppress switching-induced surges, are connected in parallel to them.

Damping resistors R_1–R_8 serve for absorbing a part of the energy that was not transferred to the load and returns to the primary storage. They are included in the discharge circuit of the capacitors after the current-direction reversal and enabling of the rectifying diodes, whose pairs D_1–D_2, ..., D_{15}–D_{16} with resistors, which are connected between them, shunt the switching thyristors T_1–T_8 in the reverse direction. At the chosen ratings of the damping resistors (C5-35-100 W, 1.5 Ω) the discharge has an aperiodic character with a time constant of ≈50 μs.

Pulses from the outputs of each of eight modules of the primary storage are transmitted to the primary winding of the pulse transformer along individual cables. The outputs of the cable lines are combined in two groups (four in each group) and connected to the collectors of two sealed lead-ins of the primary winding of the pulse transformer in the oil-filled HV unit. The use of eight cable lines reduces the inductance of primary-storage discharge circuit, and their combining only at the inputs of the pulse transformer provides

the conditions for enabling all switching thyristors regardless of the spread of their time parameters. The cable lines are made of four-conductor PVS electrotechnical wire with a cross section of the conductors of 4 mm^2. The conductors that are diametrically positioned in the cross section of wires are connected in parallel and form double-wire lines with a low linear inductance (≈180 nH/m).

The total inductance of the primary-storage discharge circuit that was measured upon short-circuiting of the transformer lead-ins does not exceed 0.35 μH for 6-m-long lines.

Design of the HV Unit of the Generator

The HV unit is manufactured in the form of a hermetically sealed cylindrical tank, inside which, in the medium of insulating transformer oil, there are a pulse transformer, the inner electrode of the HV coaxial capacitor on a base insulator, and the output sectioned insulator. On the top of the tank, the gas-filled SG switch is installed behind the output insulator, and the working electric-discharge chamber is above the SG.

The schematic diagram of the HV unit and its appearance with the removed outer cylindrical housing are shown in Fig. 2.

Pulsed HV Transformer

The transformer is one of the key elements of the facility. The high energy-conversion efficiency and the generator operation reliability were attained via the use of a transformer with a closed magnetic circuit and foil windings. In contrast to typical designs with wire windings, the foil transformer is resistant to rapid output-voltage jumps, which are inevitable in the case of nanosecond discharge times of the HV capacitor.

The transformer is manufactured on a twisted multisection magnetic conductor with a cross-sectional area of ≈80 cm^2 of 0.1-mm-thick transformer steel with an increased window (40 × 60 cm^2) for the placement of a HV winding with gradient rings that are installed on it.

The transformer primary winding contains three turns. It is made using a 300-mm-wide and 0.5-mm-thick copper strip with a double-layer interturn insulation with a 100-μm-thick Mylar film on a cylindrical base, which consists of several layers of the same film wound on the core yoke. There are terminals at both ends of the winding. The terminals from the beginning of the winding are connected to the sealed voltage lead-ins on the diametrically opposite sides of the tank, and the terminals from the winding end are connected to the tank body.

The secondary winding contains 1500 turns. It is wound with a 7-μm-thick aluminum foil with three-layer film interturn insulation (its total thickness is 24 μm) on a 130-mm-diameter polypropylene frame. The foil width is 80 mm, and the width of the interturn insulation is 280 mm. The outer diameter of the foil winding is ≈230 mm. Together with the frame and a guard electrode, which is installed over the foil winding and reduces the field strength at the edges of the extreme turns, the secondary winding is placed in a cylindrical insulating case, which is filled during impregnation with synthetic or transformer oil. A set of open gradient rings, which equalize the voltage distribution over the case surface, is installed on the outside of the case. The gradient rings are connected to the HV terminal connected to the winding end, which is positioned in the middle of the lateral (cylindrical) part of the case. Two terminals that are connected to the beginning of the winding are placed at the opposite ends of the case. Using copper strips, they are connected to the tank housing.

Because of the small radial thickness ($\Delta r \approx 50$ mm) and the use of the closed magnetic circuit, the windings have a low leakage inductance and a large coupling coefficient. The measured parameters of the transformer are as follows: the transformation ratio is $K_{tr} \approx 500$, the total leakage inductance reduced to the primary circuit is $\leqslant 0.9$ μH, and the coupling coefficient is close to 0.98.

At the chosen iron cross section and number of turns in the windings, the transformer in the analyzed circuit can operate without additional biasing. The capacitors of one of the arms are charged through the circuit that includes the primary winding of the pulse transformer. The flowing charging current magnetizes the core, thus preparing it for a working cycle of the pulse transformation during the capacitor discharge.

High-Voltage Capacitor

The capacitor is formed by two coaxial cylindrical electrodes that are insulated with transformer oil. The inner diameter of the outer electrode (case) is 1050 mm, and the diameter of the inner electrode is 910 mm. At the maximum operating voltage, the average electric-field strength in the gap is ~70 kV/cm. The total capacitance of the capacitor, including the capacitances of the end parts with adjacent elements, is $C_c \approx 1.2$ nF, which corresponds to the condition for the most efficient energy transfer from the primary circuit to the secondary one: $C_1/C_c \approx (K_{tr})^2$, where C_1 is the impact capacitance of the primary storage.

The HV electrode of the capacitor is installed on the base insulator, which, in view of the comparatively long charging time (≈45 μs), is constructed in a sectioned form (Fig. 2). It consists of five main sections and one measuring one, which is used as a capacitive divider. The sections are formed by flat metal rings

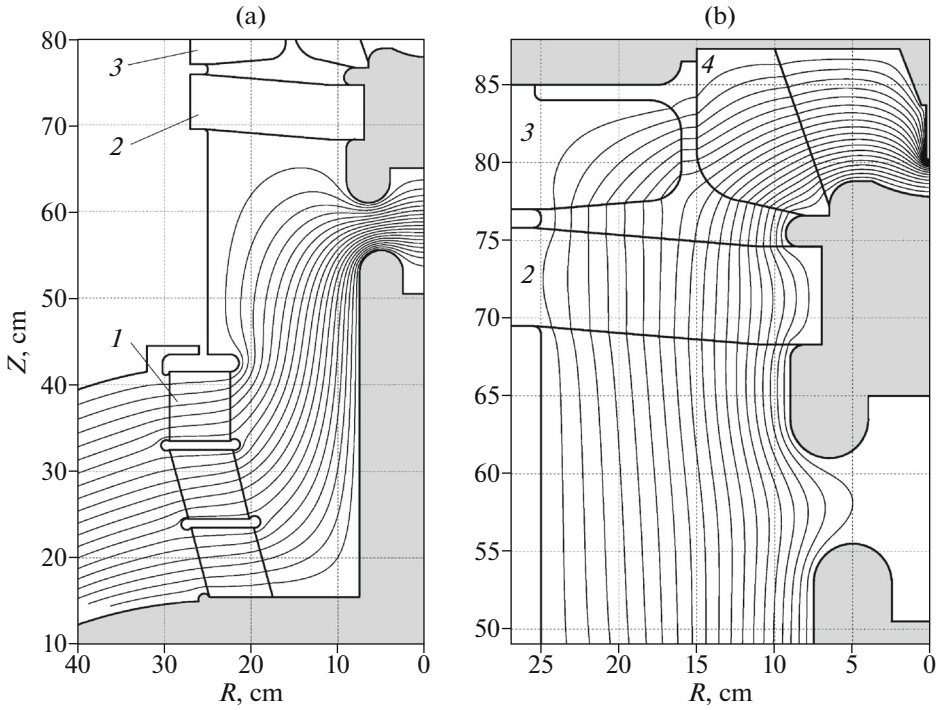

Fig. 3. The calculated pattern of equipotential lines: (a) in the region of the output insulator and the gas-filled SG (after the SG breakdown): (*1*) sectioned output insulator, (*2*) insulating diaphragm, (*3*) insert–field former, and (*4*) chamber insulator. The electrodes of the SG and chamber are shown with gray. The equipotential lines are plotted with a step of $0.05U$.

between which sets of insulating 50-mm-diameter polycarbonate inserts are mounted. The heights of the inserts in the main sections and in the measuring section are 50 and 30 mm, respectively. The capacitance of the measuring section is additionally increased by connecting a set of capacitors to it for obtaining the required voltage-division ratio. The outer and inner diameters of the rings decrease stepwise from the base ring, which is attached to the case, toward the upper ring having a socket for installing the HV electrode. The cavity inside the rings is occupied by the upper part of the pulse transformer with elements of connection of the secondary winding to the HV electrode.

Output Insulator

The insulator separates the oil-filled volume of the coaxial capacitor from the gas-filled output SG. The insulator consists of three organic-glass rings with two intermediate gradient electrodes. The geometry of the rings and the calculated distribution pattern of the electric field in the region of the insulator and SG are shown in Fig. 3.

Gas-Filled Spark Gap

The output gas-filled SG is not controlled. It is formed by two electrodes with toroidal working surfaces, one of which is attached to the output rod of the HV electrode of the coaxial capacitor and the second is attached to the insulating organic-glass diaphragm for supplying the voltage to the working chamber (Fig. 3). The SG volume is filled with nitrogen with an excess pressure of 2–3 atm. During the operation, the spark gap is blown through along a closed path in the transverse direction with a partial gas exchange and flow filtration. The hermetically sealed internal cavity of the HV electrode of the coaxial capacitor is connected to the SG chamber and used as the buffer volume, which provides the pressure stabilization in the SG region.

The SG breakdown voltage is stabilized by a pulse corona discharge, using which the gas preionization is provided in the spark gap and the operation-threshold spread, which is determined by the statistical delay time of the discharge initiation, is excluded. A corona discharge is initiated by an additional pointed electrode, which is mounted in the cavity of one of the main electrodes. The accomplished geometries of the spark and corona gaps are analogous to those proposed in [7], except for the absolute dimensions that correspond to the use of this circuit at much higher voltages. The high stability (the operation-threshold spread during long-term operation with a repetition rate of 10–50 Hz does not exceed 3%) allows the efficiency of utilizing the primary-storage energy to be

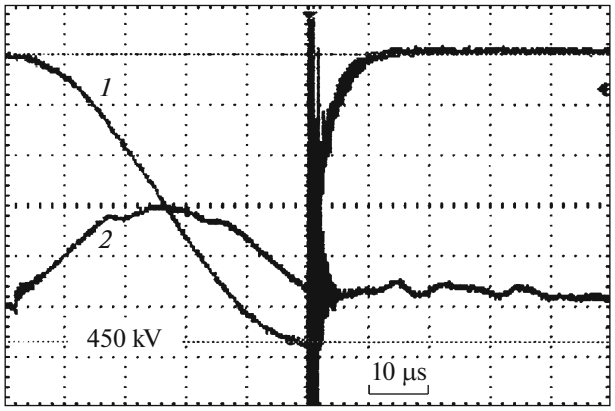

Fig. 4. Oscillograms of (*1*) the voltage across the HV capacitor and (*2*) the current in the primary circuit of the pulse transformer. The lower dotted cursor line corresponds to a voltage of 450 kV relative to the upper zero line.

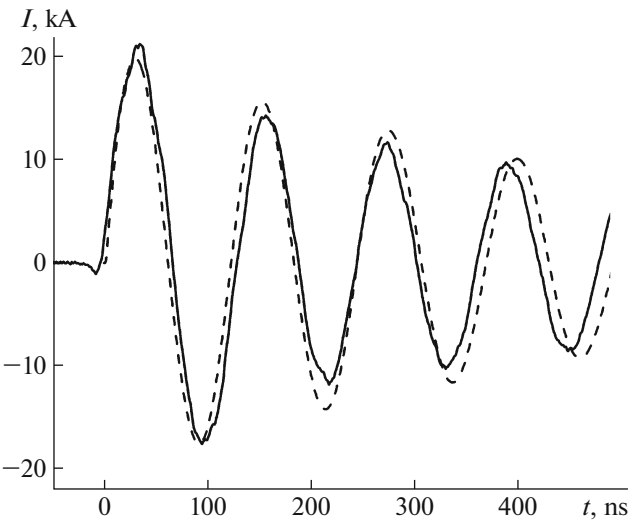

Fig. 5. An oscillogram of the discharge current upon a short-circuit in the chamber. The dashed line shows the calculated short-circuiting current; $U \approx 350$ kV.

increased owing to the chosen SG-breakdown voltage whose value is only 5–10% lower than the amplitude value of the coaxial-capacitor charging voltage.

Crushing Chamber

A schematic of one of the variants of the electric-discharge crushing chamber with a rod–plane electrode system together with the calculated electric-field distribution pattern is shown in Fig. 3b.

The working volume of the chamber is formed by a replaceable cup-shaped insulator, which is supported by the border of the HV electrode with a flat or profiled working surface and pressed from above by a cover with a unit for fastening the grounded rod electrode. The rod electrode has the form of a thread stud that allows the working gap to be controlled without opening the chamber. The region that surrounds the cup-shaped insulator is filled with deionized water for electrical insulation of the HV electrode, which is fixed on the diaphragm between the SG and the chamber. In this region, an additional circular dielectric insert—field "former"—is placed, using which a more uniform voltage distribution over the chamber insulator is attained.

The material is crushed in such a chamber in mass portions of 1–1.5 kg. A grinding cycle lasts 1–3 min depending on the required fractional composition (100–300 μm). The discharge of the ready product is performed through an outlet branch pipe by an impulse water flow that is supplied to the chamber through a separate inlet.

THE MAIN CHARACTERISTICS OF THE GENERATOR

The results that are presented below characterize the operation of the main generator units and its output parameters.

Charging of the HV Capacitor

Oscillograms of the voltage across the HV capacitor (a signal from the capacitive voltage divider) and the current in the circuit of the pulse-transformer primary winding upon a breakdown of the output SG near the voltage maximum are shown in Fig. 4. By the SG breakdown moment, the capacitor-charging current decreases virtually to zero and then remains almost constant.

These oscillograms were obtained at a charging voltage of the primary storage of 460 ± 10 V, which corresponds to an energy of 127 ± 5 J stored in it. The maximum voltage value across the HV capacitor, which is shown in the above oscillogram with the lower dotted cursor line, reaches 450 ± 10 kV, thus corresponding to an energy-transfer efficiency of 0.9 ± 0.02.

Output Pulses

An oscillogram of the discharge current upon a short circuit in the chamber and a breakdown voltage of the output gas-filled SG (the voltage across the HV capacitor) $U \approx 350$ kV is shown in Fig. 5. The current was measured with an inductive sensor that was installed outside of the dielectric insert, which serves

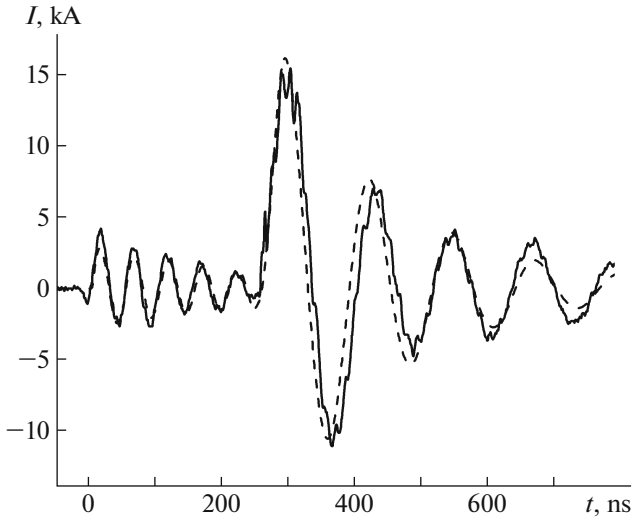

Fig. 6. An oscillogram of the discharge current through the gap $d = 25$ mm between the grounded rod electrode and the flat HV electrode in water at a voltage of $U = 350$ kV; the dashed line is the calculation.

as the field former (Fig. 3b) and encompasses a sector with an angular size of about 20°. This sensor had an external *RC* integrating chain.

Figure 5 also shows the calculated (dashed line) short-circuiting current in the chamber that was obtained within the framework of a simple electrotechnical model with fixed parameters of the *R*–*L*–*C* discharge circuit. The capacitance value was taken to be equal to the total capacitance of the HV capacitor $C_c = 1.2$ nF, the initial voltage across the capacitor was adopted to be equal to the measured $U = 350$ kV, and the inductance and ohmic resistance were varied until the best agreement with the measured current was attained. The thus found inductance value $L \approx 0.28$ μH occurs to be close to the calculated value 0.27 μH for the given geometry of the discharge circuit (the ohmic resistance is $R \approx 1$ Ω). The current half-wave duration in the short-circuiting mode is ~60 ns.

Figure 6 shows an oscillogram of the discharge current in the water-filled chamber through the gap $d =$ 25 mm between the grounded rod and flat HV electrodes for the same voltage (≈350 kV) that charges the coaxial capacitor.

The water-gap breakdown delay for the given pulse is ≈230 ns relative to the operation moment of the output gas-filled SG of the generator (in the oscillogram, $t = 0$). Current oscillations before the water-gap breakdown represent the charging process of the capacitance of the water-filled chamber. The chamber capacitance that was measured over an oscillation period is ≈250 pF. After a breakdown, the current amplitude increases to a level of above 15 кА, and the duration of the first current half-wave is ≈75 ns. The oscillation damping after the breakdown was used to determine the impedance of the discharge channel in water, which is introduced into the circuit.

The results of modeling with consideration for the obtained values of the chamber capacitance, the discharge-channel resistance, and the measurement data in the short-circuiting mode, which are locked to the gap breakdown moment, are shown with a dashed line in Fig. 6. The fraction of the sensor-recorded capacitive current before the gap breakdown is taken into account in this modeling.

CONCLUSIONS

The first pilot generator specimen was built in 2006. After tests were performed and the pulse-transformer design was improved in 2007–2008, the works on the development of two additional generators were completed. Subsequently, all three generators were used in experiments on selective fragmentation of a mineral quartz raw material in order to obtain high-purity quartz concentrates, on recycling substandard quartz-glass products, and crushing other nonconducting minerals. During experiments with the chamber for a continuous crushing cycle, the maximum duration of the continuous generator operation in a typical mode at 450 kV and 20 Hz reached 40 h and was limited by the necessity of replacing one of the chamber electrodes. The productivity of the facility in this regime was 120–130 kg/h of quartz-concentrate fractions ranging from +80 to −500 μm at the initial size of the mineral-raw material of −40 mm. During the time of the performed experiments, the service life of the first two facilities was $>10^8$ pulses without the necessity of repairing or replacing generator units.

The experience showed that the circuit and the developed design satisfy stringent requirements for pulse generators for technological electric-discharge facilities. In particular, the use of a structural capacitor with a liquid dielectric (oil) as the HV capacitor, which is discharged into the working gap of the chamber through one uncontrolled two-electrode SG, provides stable operation of the generator even under the most unfavorable conditions in the presence of discharge-current oscillations and a voltage reversal. The coaxial design of the HV capacitor, the switching SG, and the working chamber makes it possible to obtain a low output impedance of the generator discharge circuit and increase the efficiency of the energy deposition in the low-resistance discharge channel. The service life of the structural capacitor at moderate values of the electric-field strength is virtually unlimited.

The closed structure of both the HV unit and the working chamber, which is combined with it, and the placement of the generator's low-voltage-section units

in closed cabinets prevent the penetration of pulse electromagnetic fields to the environment, and the use of an electric-machine apparatus excludes the appearance of pulse interference in the mains.

REFERENCES

1. Martello, E.D., Bernardis, S., Larsen, R.B., Tranell, G., Sabatino, M.D., and Arnberg, L., *Powder Technol.,* 2012, vol. 224, pp. 209–216. DOI: 10.1016/j.powtec.2012.02.055
2. Kurets, V.I., Usov, A.F., and Tsukerman, V.A., *Elektroimpul'snaya dezintegratsiya materialov* (Electric-Pulse Disintegration of Materials), Apatity: Kol. Nauchn.Tsentr Ross. Akad. Nauk, 2002.
3. Mesyats, G.A., *Techn. Phys. Lett.,* 2005, vol. 31, no. 24, pp. 1061–1064.
4. Ushakov, V.Ya., Klimkin, V.F., Korobeinikov, S.M., and Lopatin, V.V., *Proboi zhidkostei pri impul'snom napryazhenii* (Breakdown of Liquids under Pulse Voltages), Tomsk: Nauchn.-Tekhn. Liter., 2005.
5. Lopatin, V.V., Noskov, M.D., Usmanov, G.Z., and Cheglokov, A.A., *Russ. Phys. J.,* 2006, no. 49, no. 3, pp. 243–250.
6. Kovalchuk, B.M., Kharlov, A.V., Vizir, V.A., Kumpyak, V.V., Zorin, V.B., and Kiselev, V.N., *Rev. Sci. Instrum.,* 2010, vol. 81, no. 10, p. 103506. DOI: 10.1063/1.3497307
7. Krastelev, E.G., in *Sbornik nauchnykh trudov "Nauchnaya sessiya MIFI-2006"* (Coll. Sci. Papers "Scientific Session Mos. Eng.-Phys. Inst.-2006"), Moscow: MIFI, 2006, vol. 8, p. 45.

Translated by A. Seferov